EBioMedicine 50 (2019) 211–223

Contents lists available at ScienceDirect

EBioMedicine

journal homepage: www.elsevier.com/locate/ebiom

Research paper

Serum extracellular vesicles contain SPARC and LRG1 as biomarkers of colon cancer and differ by tumour primary location

Min-Er Zhong[a], Yanyu Chen[b], Yi Xiao[a], Lai Xu[a], Guannan Zhang[a], Junyang Lu[a], Huizhong Qiu[a], Wei Ge[b,*], Bin Wu[a,*]

[a] Department of General Surgery, Peking Union Medical College Hospital, Chinese Academy of Medical Sciences and Peking Union Medical College, Beijing, China
[b] National Key Laboratory of Medical Molecular Biology & Department of Immunology, Institute of Basic Medical Sciences, Chinese Academy of Medical Sciences, Beijing, China

ARTICLE INFO

Article History:
Received 15 August 2019
Revised 3 November 2019
Accepted 4 November 2019
Available online 18 November 2019

Keywords:
Colon cancer
Extracellular vesicles
Proteomics
Metastasis
Tumour location

ABSTRACT

Background: Recently, the distinction between left- and right-sided colon cancer (LCC and RCC) has been brought into focus. RCC is associated with an inferior overall survival and progression-free survival. We aimed to perform a detailed analysis of the diversity of extracellular vesicles (EV) between LCC and RCC using quantitative proteomics and to identify for new diagnostic and prognostic biomarkers.

Methods: We isolated EVs from patients with LCC, RCC and healthy volunteers, and treated colorectal cancer cell line with serum-derived EVs. We then performed a quantitative proteomics analysis of the serum-derived EVs and cell line treated with EVs. Proteomic data are available via ProteomeXchange with the identifiers PXD012283 and PXD012304. In addition, we assessed the performance of EV SPARC and LRG1 as diagnosis and prognosis biomarkers in colon cancer.

Findings: The expression profile of the serum EV proteome in patients with RCC was different from that of patients with LCC. Serum-derived EVs in RCC promoted cellular mobility more significantly than EVs derived from LCC. EV SPARC and LRG1 expression levels demonstrated area under the receiver-operating characteristic curve values of 0.95 and 0.93 for discriminating patients with colon cancer from healthy controls. Moreover, the expression levels of SPARC and LRG1 correlated with tumour sidedness and were predictive of tumour recurrence.

Interpretation: We identified differences in EV protein profiles between LCC and RCC. Serum-derived EVs of RCC may promote metastasis via upregulation of extracellular matrix (ECM)-related proteins, especially SPARC and LRG1, which may serve as diagnosis and prognosis biomarkers in colon cancer.

Research in context

Evidence before this study

Primary tumour sidedness has been found to be prognostic in colorectal cancer, with right-sided tumours having a worse prognosis than left-sided tumours, even after controlling for known negative prognostic factors. In addition, recent analysis suggests that sidedness may also be a predictive marker of the response to epidermal growth factor receptor (EGFR) inhibitor, with right-sided tumours having a poor response.

Added value of this study

The diversity between left- and right-sided colon cancer is still controversial. And molecular underpinnings of this difference remain unclear. Here, we present a detailed analysis of the

Abbreviations: CRC, colorectal cancer; NCCN, National Comprehensive Cancer Network; LCC, left-sided colon cancer; RCC, right-sided colon cancer; mCRC, metastatic CRC; PFS, progression-free survival; EGFR, epidermal growth factor receptor; OS, overall survival; EV, extracellular vesicles; EMT, epithelial–mesenchymal transition; TMT, Tandem Mass Tagging; LC, liquid chromatography; MS, mass spectrometry; HPLC, High performance liquid chromatography; TOF, Time of Flight; GO, Gene Ontology; FDR, false discovery rate; PCA, Principal component analysis; NTA, nanoparticle tracking analysis; FBS, fetal bovine serum; ROC, receiver operating characteristic curve; AUC, area under the receiver-operating characteristic curve; DEPs, differentially expressed proteins; ECM, extracellular matrix; SPARC, secreted protein acidic and cysteine rich; LRG1, leucine rich alpha-2-glycoprotein 1; VCAM1, vascular cell adhesion molecule 1; THBS1, thrombospondin 1; FN1, fibronectin 1; VTN, vitronectin

* Corresponding authors.
E-mail addresses: wei.ge@chem.ox.ac.uk (W. Ge), wubin0279@hotmail.com (B. Wu).

https://doi.org/10.1016/j.ebiom.2019.11.003

diversity in extracellular vesicles between left- and right-sided colon cancer using quantitative proteomics. Our study confirms the difference between left- and right-sided colon cancer at the serum extracellular vesicles level.

Implications of all the available evidence

The present study identify difference between left- and right-sided colon cancer at the serum extracellular vesicles level. And we found that extracellular vesicles derived from patients with right-sided tumours promote metastasis more significantly than those derived from patients with left-sided colon cancer. We hypothesize that serum-derived extracellular vesicles from right-sided colon cancer promote metastasis by upregulation of extracellular matrix-related proteins, especially SPARC and LRG1, which may serve as potential diagnostic and prognostic biomarkers in colon cancer.

1. Introduction

It has long been recognized that colorectal cancer (CRC) is molecularly heterogeneous, and its clinical behaviour differs if the primary tumour is located in the right or left side of the colon [1,2]. According to the National Comprehensive Cancer Network (NCCN) guidelines, tumours located in the splenic flexure, descending colon, sigmoid colon, and rectum are defined as left-sided colon cancer (LCC). In contrast, tumours located in the region from the hepatic flexure to the cecum are defined as right-sided colon cancer (RCC) [3].

Over the past few years, the distinction between LCC and RCC has been brought into focus due to their diversities in biology, clinical characteristics, prognosis and treatment response [2,4,5]. Multiple retrospective analyses of randomized controlled trials [6–9] have revealed that RCC leads to an inferior prognosis. A retrospective analysis of the NCIC CO.17 trial [6] indicated that tumour location could be used to predict treatment effectiveness. In accordance with this conclusion, a retrospective analysis of CRYSTAL and FIRE-3 studies [7] indicated the value of primary tumour location in predicting metastatic CRC (mCRC), with right-sided tumours associated with a worse prognosis than left-sided tumours regardless of the first-line treatment regimen. However, with respect to progression-free survival (PFS), a significant interaction between primary tumour location and treatment was observed. Analysis of tumour location subgroup data from the Phase Ⅲ CALGB/SWOG 80405 trial [8] showed similar prognostic and predictive impacts of tumour location to those of a retrospective analysis of CRYSTAL and FIRE-3 studies. Consequently, the NCCN guidelines now recommend against using first-line epidermal growth factor receptor (EGFR) inhibitors in patients with RCC, regardless of KRAS status. To investigate the prognosis between left- and right-sided non-metastatic colon cancer, we performed a retrospective study of 175 patients with histologically proven stage Ⅲ colon cancer undergoing radical resection at our institute from 2005 to 2012. Our study [10] demonstrated that patients with a right–sided tumour carried a greater number of negative prognostic factors such as mucinous adenocarcinoma, and had inferior overall survival (OS) and PFS compared with those with tumours originating on the left side. In another retrospective study of 1,869 patients with stage Ⅲ colon cancer [11], patients with right-sided tumours had shorter survival after relapse and shorter OS compared with the patients with left-sided tumours. A more comprehensive understanding of the biological differences between tumours in different locations may help to develop more efficacious therapies. Further research is now required to clarify the reasons for these differences and to identify better treatments tailored to the patient. We believe that there are molecular characteristics that can be used to track right versus left disease, although they are not yet well described.

Recently, the roles of extracellular vesicles (EV) and their contents as potential contributors to oncogenesis, metastatic disease, and resistance to chemotherapy is a rapidly expanding area of research in cancer biology [12,13]. EVs are extracellular vesicles released from the cell membrane that play a critical role in cell-cell communication [14] through the transmission of molecular messengers that alter the phenotype of recipient cells [15,16]. Previous studies have indicated that EVs are involved in metastasis by harbouring molecules that are involved in the epithelial-mesenchymal transition (EMT) or preparing target tissues for metastasis [17,18]. In general, previous studies of EVs at the levels of basic and clinical research are important in elucidating their role in cancer.

To date, most studies of vesicle-mediated carcinogenesis were performed with EVs isolated from supernatants of tumour cell lines and, less frequently, from serum of patients with cancer. Here, we present the first detailed analysis of the diversity in EVs between LCC and RCC using quantitative proteomics. The procedure is schematically outlined in Fig. 1.

2. Materials and methods

2.1. Reagents

Details of reagents are given in Supplementary Materials and Methods.

2.2. Patients and serum samples

A total of 78 patients diagnosed with stage Ⅲ moderately differentiated colon cancer and 40 healthy volunteers were recruited in Peking Union Medical College Hospital (PUMCH, Beijing, China) from 2015 to 2017. The following exclusion criteria were applied: (a) with diabetes, autoimmune diseases, or blood diseases; (b) with a history of chemo- or radiotherapy, or a previous history of malignancy; (c) transverse colon cancer; (d) rectal cancer; (e) mucinous adenocarcinoma. The definition of LCC and RCC is consistent with that described in the Introduction. Rectal cancer was not included in the present study because they are treated differently to colon cancer. There was no statistical difference between these two patient groups. Details are shown in Table S1. All patients with stage Ⅲ colon cancer were treated with an oxaliplatin-based chemotherapy regimen followed by curative resection. Long-term follow-up was performed according to the NCCN guidelines [19]. The patients' follow-up cut-off was January 2019. The healthy volunteers were recruited from people that had their medical check-up in our centre. Most of them underwent a thorough physical exam, electrocardiography, some laboratory tests, such as complete blood count and serum tumour marker tests, as well as medical imaging such as chest X-ray and abdominal ultrasound. They were defined as healthy individuals according to their check-up results. An additional 75 patients with other malignancies including thyroid cancer ($n = 25$), cervical cancer ($n = 25$) and gastric cancer ($n = 25$) enrolled for validation in March 2019.

Clinical information about patients and volunteers are shown in Table S1-4. This study was approved by the Ethics Committee of PUMCH (No. S-k655) and was conducted in accordance with the most recent version of the Declaration of Helsinki. All patients and healthy volunteers provided written informed consent to participation in this study.

Venous blood samples were obtained (using a 21 G gauge needle; the first 1 ml was discarded) from both patients and healthy volunteers in the fasting state. Serum samples were collected from patients before they underwent radical surgery. For quantitative proteomics analysis, serum samples from 14 patients with LCC and 14 patients with RCC were pooled, respectively. Serum samples obtained from

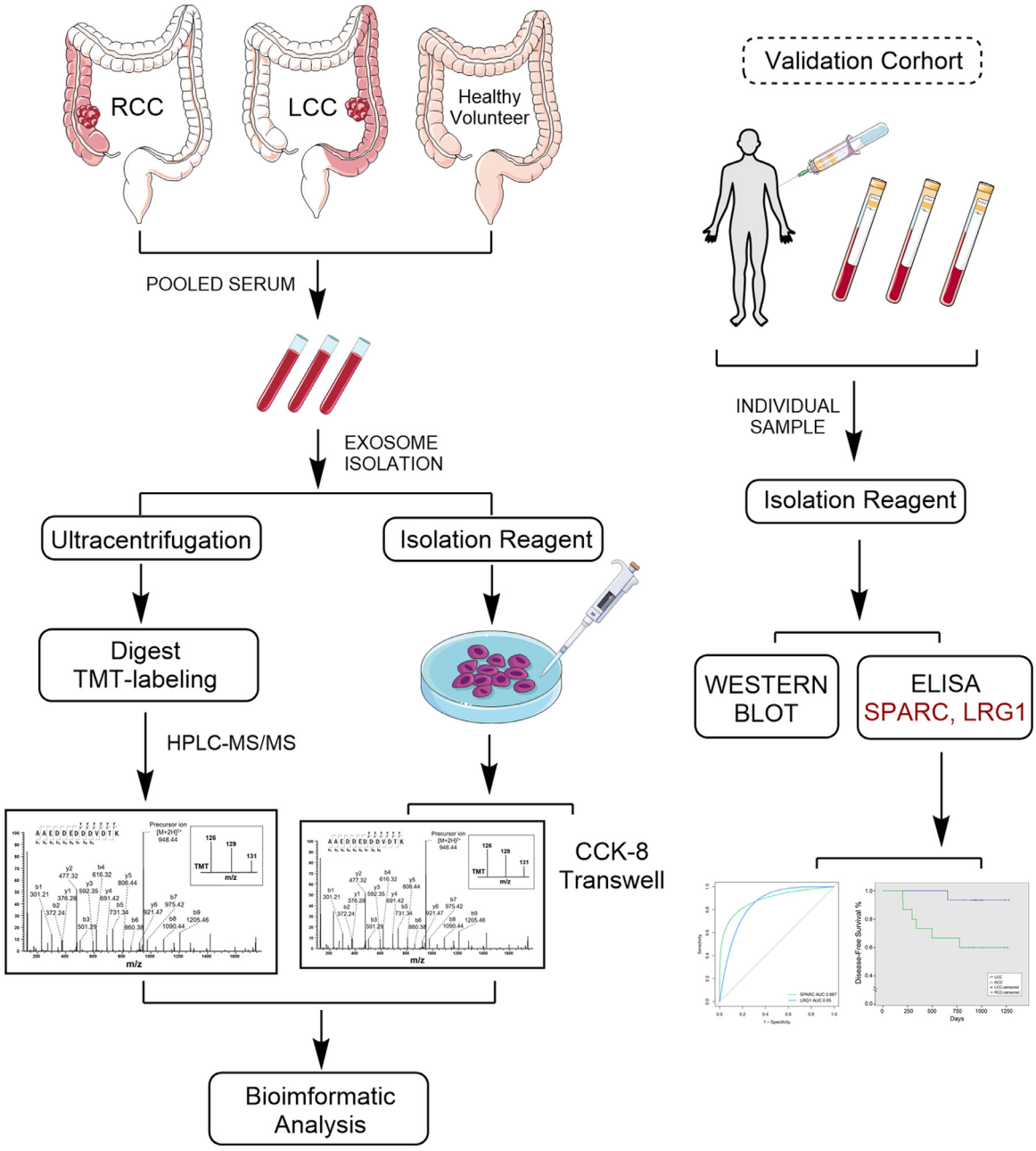

Fig. 1. Schematic workflow. The workflow shown the TMT-based quantitative proteomic analysis of extracellular vesicles (EV) isolated from the pooled serum of patients with colon cancer and healthy volunteers. "RCC" refers to right-sided colon cancer; "LCC" refers to left-sided colon cancer. Original elements used in this diagram are from Servier Medical Art (http://smart.servier.com/).

15 healthy volunteers were pooled and allocated to the normal control group. These three groups of pooled serum were applied to EV isolation by ultracentrifugation. Serum samples from the rest patients and volunteers were used for validation.

2.3. EV isolation from human serum

EV were isolated from serum samples by ultracentrifugation or Total Exosome Isolation Reagent. For proteomics analysis, serum samples were pooled respectively and then applied to ultracentrifugation as previously described [20]. A detailed description of ultracentrifugation experiments is given in Supplementary Materials and Methods. Due to the low volumes of sera available from patients, we isolated EV using Total Exosome Isolation Reagent for other assays according to the manufacturer's instructions. In brief, pooled or individual serum samples were first diluted with an equal volume of PBS to decrease viscosity, followed by the addition of 0.2 vol of the Total Exosome Isolation Reagent. Mixtures of serum and reagent were vortexed and incubated at 4 °C for 30 min and then centrifuged at room temperature to isolate EV pellets. Samples were centrifuged at 10,000 × *g* for 30 min and the pellet was then resuspended in PBS containing 1% penicillin/streptomycin. EVs isolated from 100 μL serum were resuspended in 20 μL PBS. The protein content of the isolated EV was measured using the BCA assay after lysis with RIPA.

2.4. Tandem mass tagging (TMT) labelling

For TMT labelling, the lysates of EVs from the three sample groups (Normal, LCC and RCC) were diluted to 1 mg/mL with 8 M urea. Labelling was performed using the TMT kit according to the manufacturer's

protocol with slight modifications. Details are described in Supplementary Materials and Methods.

2.5. Liquid chromatography (LC)-mass spectrometry/mass spectrometry (MS) analysis

The TMT-labelled peptides were fractionated by High performance liquid chromatography (HPLC). For LC-MS/MS analysis, peptides were separated using a 135-min gradient elution at a flow rate 0.3 μL/min with the Ultimate U3000 system, which was directly interfaced with the Thermo Orbitrap Fusion Lumos mass spectrometer. A detailed description of HPLC and LC-MS/MS experiments is given in Supplementary Materials and Methods.

2.6. Data processing

Proteins were identified using Proteome Discoverer 2.2 software (Thermo Scientific) with the SEQUEST search engine. The raw MS data files were searched against the UniProt/SwissProt human proteome database (released on February 5, 2018). The search criteria and details are described in Supplementary Materials and Methods. In the current study, identified proteins were defined as proteins with at least two unique peptides.

2.7. Protein identification using MS/MS data

Representative MS/MS spectral identification was performed as previously described [21]. Briefly, MS/MS spectral data of identified peptides and the intensity of TMT precursor ions were used for protein quantification. The masses of the resulting peptides were measured to obtain a Time of Flight (TOF) spectrum. Peaks from the TOF spectrum were selected for sequencing by fragmentation (MS/MS).

2.8. Bioinformatics analysis

For proteomic analysis of human serum-derived EVs, relative protein abundances were presented as the ratios to TMT-129/131 (LCC/normal group), 126/131 (RCC/normal group), and 126/129 (RCC/LCC). The differential expression threshold was set as a 1.5-fold change. Details of the MS proteomics data are available from the ProteomeXchange Consortium [22] via the PRIDE partner repository (dataset identifier PXD012283). For proteomic analysis of CRC cell line SW480 treated with serum-derived EVs, relative protein abundances were presented as the ratios to TMT-127/126 (normal/PBS group), 129/126 (LCC/PBS group), 131/126 (RCC/PBS group), 129/127 (LCC/normal group), 131/127 (RCC/normal group), and 131/129 (RCC/LCC). Proteins were considered differentially expressed when fold change >1.2. The MS proteomics dataset was submitted to the ProteomeXchange Consortium with the identifier PXD012304. To stratify the proteome, a list of cancer-related proteins was downloaded from The Human Protein Atlas database (https://www.proteinatlas.org/) [23]. Gene Ontology (GO) functional enrichment analysis was conducted using the clusterProfiler package [24] in R program (R Foundation for Statistical Computing, Vienna, Austria. http://www.R-project.org/). False discovery rate (FDR) <0.05 was set as the threshold for statistical significance for GO enrichment analysis. Pathway enrichment analysis was performed using the Cytoscape plug-in ClueGO [25] based on WikiPathway database (released: November 05, 2018). Statistical significance of pathways was based on adjusted *P*-values of <0.05 and the presence of at least five target genes. Hierarchical Ward-linkage clustering was performed based on Spearman correlation coefficients using JMP Pro (version 13.0, SAS Institute, Cary, NC, USA). Principal component analysis (PCA) was performed using JMP Pro. The STRING database (http://string-db.org) [26] was introduced for protein-protein interaction network analysis. And the results were graphically represented with Cytoscape (version 3.2.1, Cytoscape Consortium, USA, https://cytoscape.org/) [27].

2.9. Nanoparticle tracking analysis (NTA)

The size distribution and concentration of EV were calculated by NTA using a Nanosight LM10 (Nanosight, Amesbury, UK) equipped with a fast video capture and particle tracking software. Nanoparticles were illuminated by a 635 nm laser and their movement under Brownian motion was record for 60 s. Then videos were collected and analysed with NTA 3.2 software (Nanosight, Amesbury, Wiltshire, UK).

2.10. Western blotting analysis

Serum EV and primary tumour tissue were applied for immunoblotting. Western blot analyses were performed with the following primary antibodies: ALIX, CD63, TSG101, PSMA5, HMGB1, SPARC and LRG1. Details are described in Supplementary Materials and Methods. Coomassie-stained SDS-PAGE was used as loading control for EV. Human β-actin was used as an internal reference for tissue proteins. Densitometry analysis was performed using the ImageJ software (National Institutes of Health, USA).

2.11. ELISA

For each target protein detection, 300 μL serum-derived EVs were resuspended in 70 μL RIPA and diluted to 100 μL with sample diluent provided in the ELISA kit. The procedure was performed following the manufacturer's instruction with no modifications.

2.12. Cell culture

SW480 and HCT116 cells were obtained from China Infrastructure of Cell Line Resources (Beijing, China). Cell line authentication and mycoplasma testing were not performed. SW480 was cultured in Dulbecco's Modified Eagle Medium (DMEM) containing 10% fetal bovine serum (FBS). HCT116 was cultured in Iscove's modified Dulbecco's medium (IMDM) containing 10% FBS. All cell cultures were maintained at 37 °C under at 5% CO_2 in a humidified atmosphere. Cells were passaged approximately every 2–3 days.

2.13. Cell proliferation assay

Cells (2×10^3) were seeded into 96-well plates with medium contained 40 μg EVs. Cell growth was determined every 24 h by using the Cell Counting Kit-8 (CCK-8) assay. Three replicates per condition were assayed.

2.14. Cell invasion and migration assay

Transwell assays were used for studying the motility of cells treated with serum EVs as previously described [20]. Briefly, 175 μg EVs isolated from serum of colon cancer patients or healthy volunteers were added to the upper chamber transwell insert; an equal volume of EV-free PBS was added as the blank control. More details are described in Supplementary Materials and Methods. At first, EVs isolated from pooled samples were applied for transwell assays. Then, we performed a further validation using another group of individual samples. We randomly selected four healthy volunteers, four patients with LCC, and four patients with RCC from the validation cohort. None of these 12 individuals were included in the previous analysis of pooled samples. These 12 individuals were allocated to four groups. Each group included one healthy control, one LCC sample, one RCC sample and one PBS as a blank control. In other words, these 12 individuals were regarded as four groups of biological replicates.

2.15. Statistical analysis

All statistical analyses were performed with SPSS statistics (version 23.0, International Business Machines Corp., Armonk, New York, USA), JMP Pro, and GraphPad Prism (version 7.04; Nashville, TN, USA). Continuous variables are expressed as the mean ± SD. Differences between groups were compared using Student's *t*-test. Receiver-operating characteristic (ROC) analysis was used to assess the specificity and sensitivity of the biomarkers and the area under the ROC curve (AUC) was estimated for each individual protein. The Kaplan–Meier curves were generated to analyse the cumulative probability of PFS and statistical significance was evaluated using log-rank tests. The Cox proportional hazards regression was carried out to identify proteins with expression correlating with PFS. The Benjamini–Hochberg procedure was used to control the FDR. $P < 0.05$ (two-sided) was considered to indicate statistical significance.

3. Results

3.1. Verification of serum EV isolation

Under transmission electron microscopy, serum-derived EVs showed typical cup-shaped round morphology (Fig. S1a). The commonly reported EV-enriched surface markers ALIX, CD63 and TSG101 were detected by Western blot analysis in biological replicates for both groups (LCC, RCC and healthy controls; Fig. 2a). These vesicles showed high concentrations of ALIX, CD63 and TSG101 compared to the whole serum and supernatants of pooled serum samples after ultracentrifugation. Further verification of successful EV isolation was performed by proteomic detection of EV-enriched markers including CD9, CD63, CD81 and ALIX. Among the identified EV proteins, there was an overlap with 843 proteins (83.7%) in the ExoCarta protein list (http://www.exocarta.org, release date: July 29, 2015) (Fig. 2c). Of the top 100 exosome-associated proteins from Exocarta, 92% were identified in the present study (Fig. S1b). Analysis of the serum EV size by NTA revealed slightly lower EV size in the RCC group versus the LCC group (Student's *t*-test, $P < 0.05$; Fig. 2d-e). There were no differences in serum EV concentrations between LCC patients and healthy controls; however, the concentrations were slightly higher in LCC patients than in RCC patients (Student's *t*-test, $P < 0.05$; Fig. 2d-e). According to GO classification, most of the EV proteins identified were derived from the cytoplasmic vesicle lumen, with important molecular functions in cell adhesion molecule binding, cadherin binding, and glycosaminoglycan binding as well as the biological processes of neutrophil activation and extracellular structure organization; these categories are consistent with the reported functions of EVs (Fig. S1c-e; a complete list of all GO terms is shown in Table S5).

3.2. LCC- and RCC-derived serum EVs present distinct proteomic profiles

The protein composition of EVs isolated from serum samples of RCC and LCC patients and healthy individuals was determined using TMT-based quantitative MS technology. The MS raw data was processed by Proteome Discoverer (version 2.2). In total, 1,007 proteins were identified (Table S6).

PCA revealed differences in the proteome profiles between RCC, LCC and normal controls (Fig. 3a). With a 1.5-fold change cut-off were regarded as differentially abundant in EVs, a total of 930 proteins were found to be differentially expressed in colon cancer versus normal controls, and 495 proteins were identified as differentially expressed proteins (DEPs) in RCC versus LCC. Among the 495 DEPs identified in serum-derived EVs isolated from RCC patients relative to those from the LCC patients, 57 were upregulated and 438 were downregulated (Fig. 3b). Nineteen percent of these DEPs were cancer-related proteins (Fig. 3c).

To demonstrate the distinctions in expression levels among EV proteins in the RCC and LCC groups, hierarchical clustering analysis was performed and heatmap was generated. Information about proteins in each cluster is shown in Table S7. Using EVs from healthy volunteers as a control group, pairwise comparisons revealed that the proteomic variation profiles in RCC patients were distinct from those in LCC patients. In the RCC group, the expression of proteins in Cluster 1 was notably higher than that in the LCC and normal groups (Fig. 3d).

3.3. Functional analysis of DEPs between RCC and LCC

The heatmap presentation of the clustering results demonstrated that most of the upregulated DEPs were enriched in Cluster 1. Further GO analysis revealed that these DEPs are related mostly to biological processes of extracellular matrix (ECM) organization, epithelial cell migration, and regulation of angiogenesis (Fig. 3e; a complete list of all GO terms is shown in Table S5). In other words, proteins associated with ECM organization, epithelial cell migration and regulation of angiogenesis were upregulated in both LCC and RCC, although the upregulation was much more remarkable in RCC. Among these upregulated ECM-related proteins, we identified some glycoproteins and proteoglycans that are closely related to tumours. In particular, secreted protein acidic and cysteine rich (SPARC) and leucine rich alpha-2-glycoprotein 1 (LRG1), both of which have been reported to be associated with colon cancer [28,29] (Fig. S1f).

To gain insight into the potential role the sidedness DEPs (126/131) may play in modulation of tumour progression, Wikipathway analysis were performed on all 495 DEPs using the Cytoscape plug-in ClueGO (mapped gene numbers >5; Table S8). The sidedness DEPs were predominantly enriched in multiple cancer-related pathways, such as the PI3K-Akt signalling pathway, TGF-β signalling pathway, senescence and autophagy in cancer, and ferroptosis (Fig. 3f).

To further place the identified proteins in the context of known protein-protein interactions and gain insights into the coordinated roles of these proteins, we investigated the interactions between all cancer-related sidedness DEPs using the online resource STRING. Protein-protein interactions networks were visualized by Cytoscape according to their STRING score. An intricate network of protein-protein interactions is shown in Fig. 3g. Finally, three ECM-related proteins, SPARC, vascular cell adhesion molecule 1 (VCAM1) and thrombospondin 1 (THBS1), were identified as hub proteins of this comprehensive protein-protein network.

3.4. RCC-derived EVs promote cellular invasion and migration more significantly than LCC-derived EVs

Transwell assays showed that serum-derived EVs from both LCC and RCC patients (pooled serum) promoted the cellular motility of SW480 and HCT116 cells, although RCC-derived EVs had a greater effect than those obtained from LCC patients (Student's *t*-test, $P < 0.05$; Fig. 4a). And the further validation using different individual samples recached a similar conclusion (Fig. S2). However, neither RCC-derived EVs nor LCC-derived EVs promoted the proliferation of CRC cell lines (Student's *t*-test, $P > 0.05$; Fig. 4b). These results indicated that EVs derived from RCC contain more factors that are capable of promoting metastasis.

3.5. Verification of protein expression levels by Western blot, ELISA and representative MS/MS spectral identification

To validate the proteomics data, we chose four proteins (SPARC, LRG1, THBS1 and fibronectin 1 (FN1)) for representative MS/MS spectral identification, three proteins (SPARC, PSMA5, HMGB1) for Western blot analysis and two proteins (SPARC, LRG1) for ELISA. The representative mass spectral data were consistent with the proteomics data (Fig. S3). Independent Western blot analysis of serum

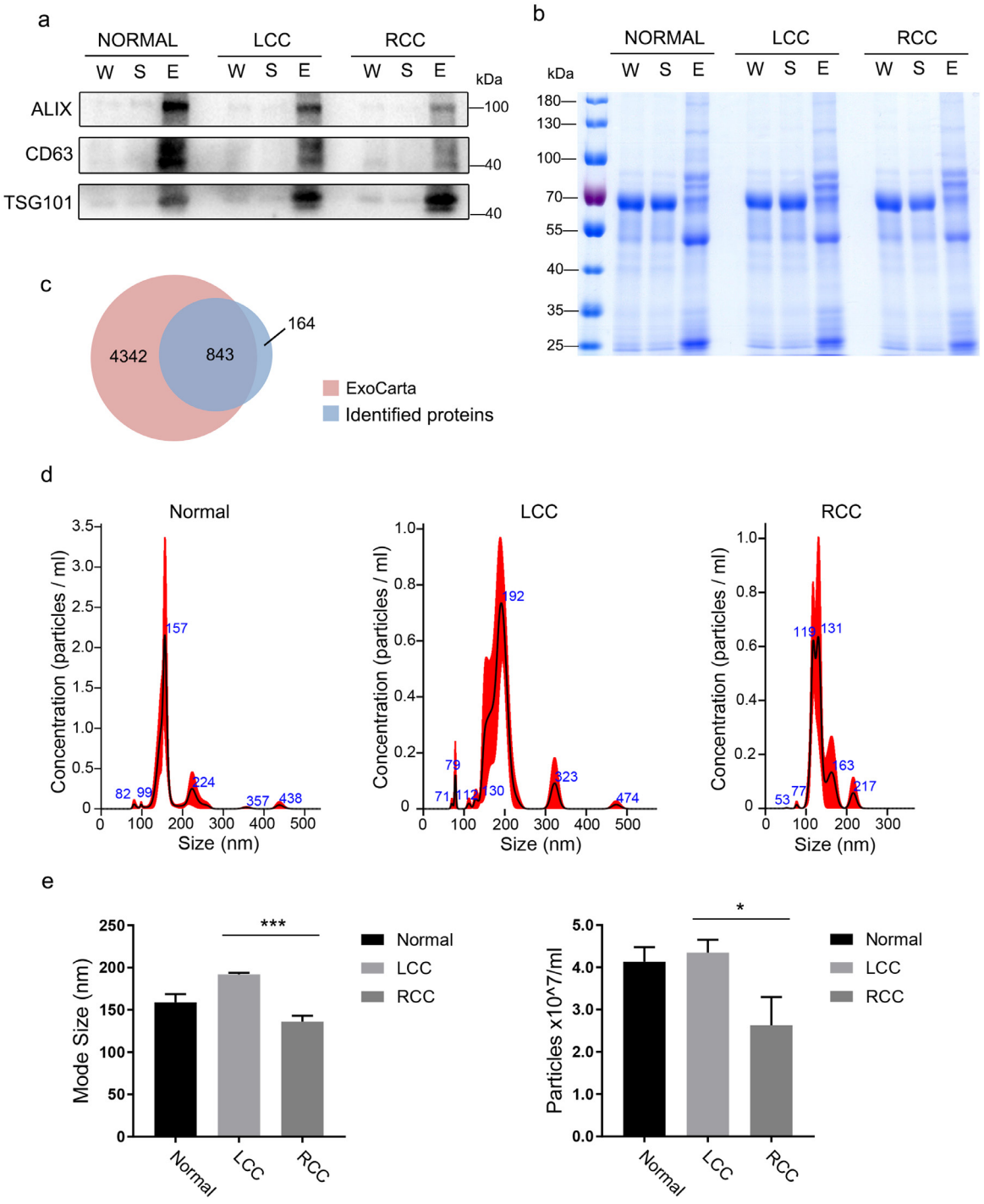

Fig. 2. Verification of extracellular vesicles (EV) isolated from pooled serum. (a) Immunoblot analyses confirmed the presence of EV markers ALIX, CD63 and TSG101 among the harvested proteins. W: whole serum. S: supernatants after ultracentrifugation. E: extracellular vesicles. (b) The Coomassie-stained SDS-PAGE of EV lysates as a loading control for (a). (c) Venn diagram showing the overlap of identified proteins with ExoCarta proteins. (d-e) Nanoparticle tracking analyses of serum EVs. "Normal" refers to healthy volunteers, "LCC" refers to left-sided colon cancer, "RCC" refers to right-sided colon cancer. *** $P < 0.001$. * $P < 0.05$ (Student's *t*-test).

samples from another 12 colon cancer patients and three normal volunteers were performed. Bands of Western blot were analysed using ImageJ software for densitometric data. Although the Western Blot data shown a trend consistent with our MS data (Fig. 5a), the densitometric analysis revealed that not all the differences were statistically significant. Only the difference of PSMA5 between LCC and RCC (Student's *t*-test, $P < 0.05$; Fig. 5b) and the difference of HMGB1 between LCC and normal control (Student's *t*-test, $P < 0.01$; Fig. 5b) were statistically significant, the remaining differences between groups were merely trending. In addition, we determined SPARC and LRG1 in the matched primary tumour tissue and the corresponding normal tissues. Immunoblot analyses confirmed upregulation of SPARC and LRG1 in tumour tissue compared to the levels in corresponding normal tissue (Fig. 5d). Similar to above, SPARC and LRG1 were both upregulated in RCC compared with LCC, but these differences were not statistically significant (Student's *t*-test, $P > 0.05$; Fig. 5e).

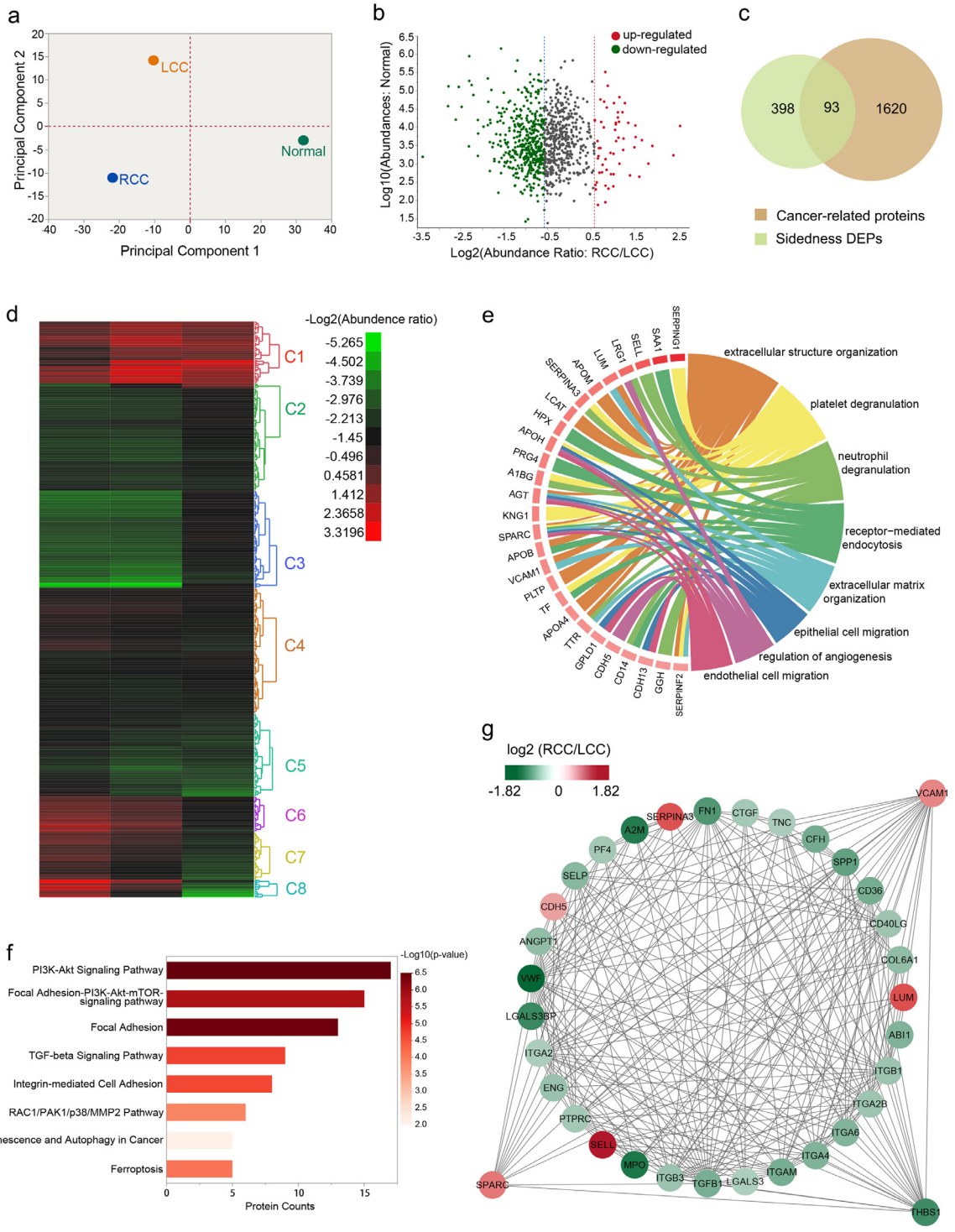

Fig. 3. Comparative analysis of proteome expression profiles of serum EV from LCC, RCC and healthy individuals. (a) Principal component analysis revealed differences in the proteome profiles between RCC, LCC and normal controls. "LCC" refers to left-sided colon cancer. "RCC" refers to right-sided colon cancer. "Normal" refers to healthy volunteers. (b) Scatter plot showing the distribution of up-regulated (red dots) and down-regulated (green dots) differentially expressed proteins (DEPs). (c) Venn diagram showing the overlap of the group of DEPs between the LCC and RCC groups (TMT-126/129) with the cancer-related proteins. (d) Hierarchical clustering analysis and heatmap of DEPs. The heatmap was constructed based on a log2 transformation of relative abundance ratios. (e) GO analysis of the upregulated proteins enriched in Cluster 1. "C1"- "C8" refers to Cluster 1 - Cluster 8. (f) Pathway analysis of the sidedness-related DEPs (TMT-126/129) of serum EVs. (g) The cancer-related DEPs in the protein-protein interaction networks are shown as nodes (MS data presented as the ratios to 126/129 were matched to STRING networks). Up- or downregulation of identified proteins is indicated by colours in the networks (upregulated in red, downregulated in green). (For interpretation of the references to colour in this figure legend, the reader is referred to the web version of this article.)

3.6. SPARC and LRG1 are related to colon cancer diagnosis and disease progression

According to the MS analyses, SPARC and LRG1 were significantly more abundant in RCC-derived EVs than in EVs derived from LCC. The results of bioinformatics analyses prompted us to investigate the contribution of SPARC or LRG1 to the clinical characteristics or progression of colon cancer. To address this issue, serum samples from 125 patients with malignancies and 25 healthy volunteers were analysed by ELISA. The ELISA data confirmed that both SPARC and LRG1 were elevated in

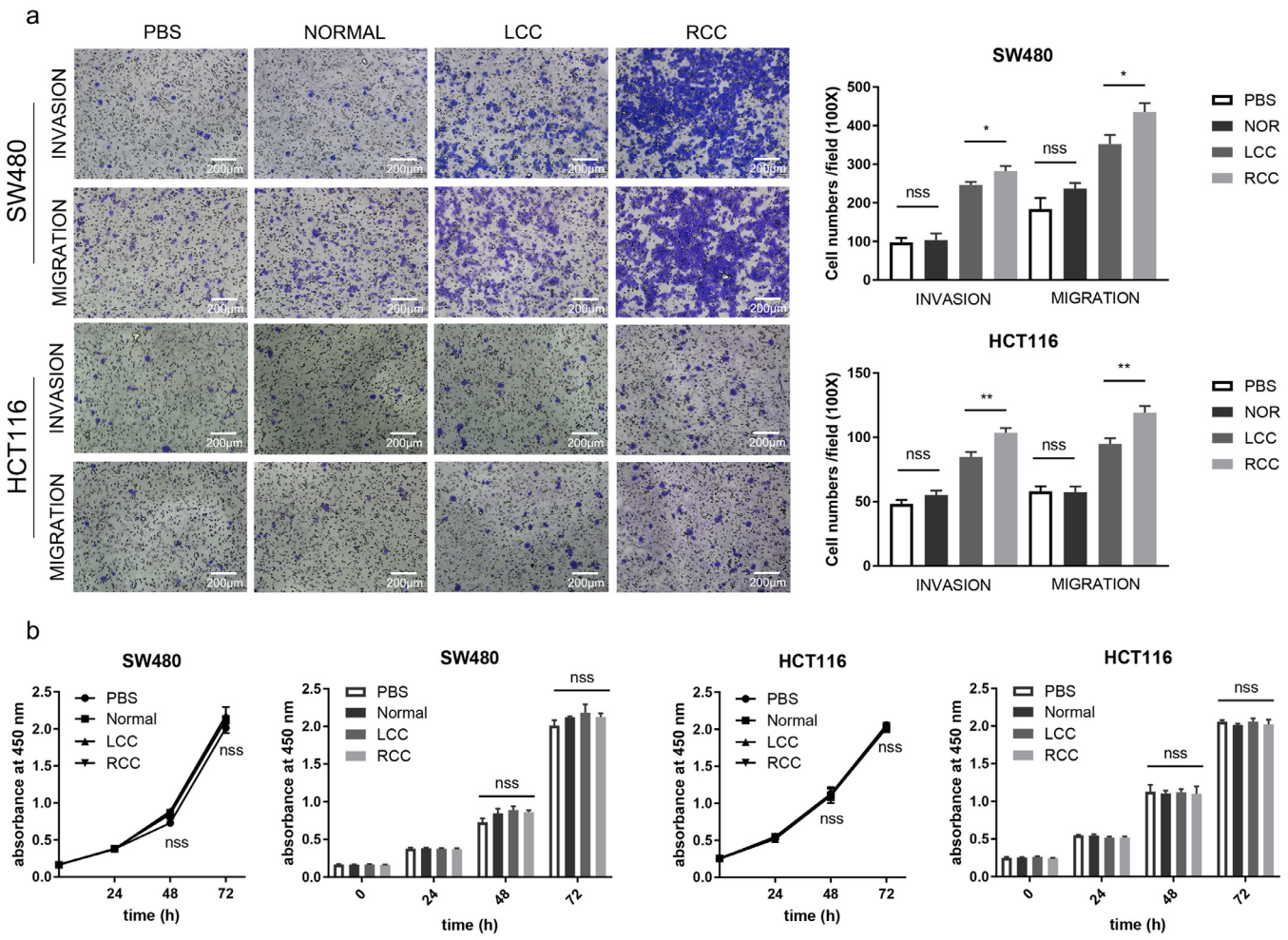

Fig. 4. Serum EV derived from colon cancer promote cellular mobility, but do not affect cellular viability. (a) Transwell assays were used to evaluate the invasion and migration of SW480 and HCT116 cells treated with serum EVs derived from LCC (pooled samples of 14 patients), RCC (pooled samples of 14 patients), and healthy volunteers (pooled samples of 15 volunteers); PBS was used as negative control. Representative photographs are shown in the left panel. The scale bar is 200 μm. Quantification of migrated cells are shown in the right panel. Data were shown as mean ± SD of two independent replicates; ** $P < 0.01$, * $P < 0.05$, nss (not statistically significant): $P > 0.05$ (Student's *t*-test). "NORMAL" refers to healthy volunteers, "LCC" refers to left-sided colon cancer, "RCC" refers to right-sided colon cancer. (b) Proliferation rates determined using the Cell Counting Kit-8 (CCK-8) method show that there were no significant differences in the proliferation of SW480 and HCT116 cells treated with serum EVs derived from left-, right-sided colon cancer patients, and healthy volunteers. nss: $P > 0.05$ (Student's *t*-test).

colon cancer patients compared to healthy volunteers. Moreover, RCC-derived EVs contained a significantly higher level of SPARC and LRG1 compared to those derived from LCC (Student's *t*-test, $P < 0.05$; Fig. 5f). No significant differences were observed in serum EV SPARC and LRG1 between patients with thyroid cancer, cervical cancer, gastric cancer and healthy volunteers (Student's *t*-test, $P > 0.05$; Fig. 5f). The ROC curve of sensitivity versus (1-specificity) were further performed to evaluated the performance of serum EV SPARC and LRG1 as biomarkers for colon cancer. The diagnostic performances of EV SPARC and LRG1 for colon cancer were excellent, with AUC values of 0.95 and 0.93, respectively (Fig. 5g). For other malignancies, the ROC curve indicated that neither serum EV SPARC nor LRG1 can be used to successfully differentiate individuals with thyroid cancer, cervical cancer or gastric cancer from healthy individuals (Fig. S4). Moreover, the serum SPARC and LRG1 were also determined. Both SPARC and LRG1 were detected in serum; however, the expression levels were significantly different from those in EV (Fig. S5). Thirty colon cancer patients were followed-up. The Kaplan–Meier survival analysis indicated inferior PFS among RCC patients compared with LCC patients (log-rank test, $P < 0.05$, Fig. 5h). The variables including sex, age, tumour location, serum levels of EV SPARC and EV LRG1 were applied for further multivariate analysis using the Cox proportional hazards model. As a result, SPARC (observed range: 2.5–23.8 ng/mg; HR: 1.73; 95% CI: 1.16–2.58; $P < 0.05$) and LRG1 (observed range: 21.8–80.6 ng/mg; HR: 1.16; 95% CI: 1.05–1.30; $P < 0.05$) were implicated as independent prognostic factors for recurrence (Fig. 5i).

3.7. Cell line treated with different EVs present distinct proteomic profiles

To investigate the effect of serum-derived EVs on a CRC cell line, SW480 cells were treated with EVs derived from LCC, RCC, normal volunteers and PBS control. We then performed TMT-based quantitative MS proteomics analysis with these samples as described previously. Finally, a total of 3,053 proteins were identified. PCA indicated distinctions in the proteome profiles between the RCC, LCC, normal control and PBS groups (Fig. 6a). With a 1.2-fold change cut-off, a total of 701 proteins were found to be differentially expressed in the EV-treated group versus PBS controls, and 139 proteins were identified as DEPs between the RCC-derived EV group versus the LCC-derived EV group (Fig. 6b). The relative abundances of these proteins are listed in Table S9. And the top ten DEPs were shown in Table 1.

3.8. Functional analysis of DEPs indicated that EVs promote EMT in a CRC cell line

GO analysis revealed that these DEPs are related mostly to the following categories: biological processes of RNA splicing, mRNA

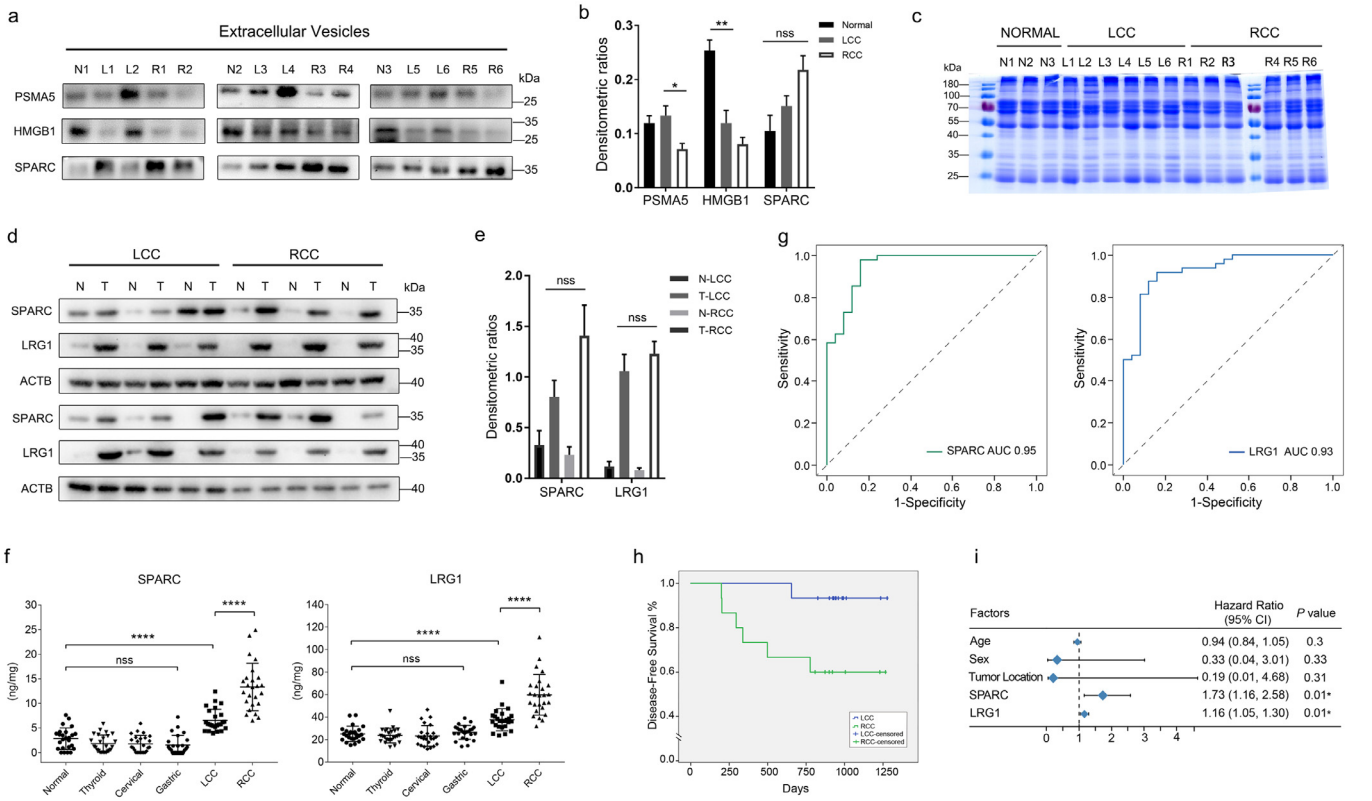

Fig. 5. Verification of protein expression, and translational relevance of EV SPARC and LRG1. (a) Validation of MS/MS data by Western blot analysis of individual samples. "N1–N3", "L1–L6", "R1-R6" represent the serum-derived EVs of individual normal volunteers and left- and right-sided colon cancer patients, respectively. (b) The optical density of each immunoreactive band was normalized with Coomassie stain. The densitometric ratios are shown in the histogram. * $P < 0.05$, ** $P < 0.01$, nss: $P > 0.05$ (Student's t-test). (c) The Coomassie-stained SDS-PAGE as the loading control for (a). LCC: left-sided colon cancer. RCC: right-sided colon cancer. (d) Western blot analysis confirmed upregulation of SPARC and LRG1 in tumour tissue compared to the levels in corresponding normal tissue. Human β-actin was used as an internal reference. N: Normal tissue. T: tumour tissue. (e) The densitometric ratios of (d). nss: $P > 0.05$ (Student's t-test) (f) Serum EVs of patients with LCC ($n = 25$), RCC ($n = 25$), thyroid cancer ($n = 25$), cervical cancer ($n = 25$), gastric cancer ($n = 25$) and healthy volunteers ($n = 25$) were analysed by ELISA using antibodies for the specific detection of SPARC and LRG1. nss: $P > 0.05$, **** $P < 0.0001$ (Student's t-test). (g) The diagnostic performances of EV SPARC and LRG1, measured by AUC, were 0.95 and 0.93, respectively. (h) The Kaplan–Meier survival analysis demonstrated that patients with RCC had inferior progression-free survival than patients with LCC. (i) Cox proportional-hazards model indicated that SPARC (HR: 1.729; 95% CI: 1.158–2.579; $P < 0.01$) and LRG1 (HR: 1.164; 95% CI: 1.047–1.293; $P < 0.01$) were independent prognostic factors of tumour recurrence. * $P < 0.05$.

processing, cell cycle checkpoint and autophagy; Molecular functions of cell adhesion molecule binding and catalytic activity; and Cellular components of cytoplasmic region and actin cytoskeleton (Fig. 6c; a complete list of all GO terms is shown in Table S5).

WikiPathway enrichment analysis revealed that these cellular DEPs were predominantly enriched in multiple cancer-related pathways such as the VEGFA-VEGFR2 signalling pathway, EMT in CRC, and the TNF alpha signalling pathway (Fig. 6d, Table S8). The pathway of EMT in CRC was visualized using Cytoscape software. Compared to the PBS control, FN1 was significantly upregulated in SW480 cells treated with LCC-derived EVs. In SW480 cells treated with RCC-derived EV, not only was FN1 upregulated, but also vitronectin (VTN) compared to the levels in the PBS control (Fig. 6e). It can be inferred that serum-derived EVs from colon cancer patients may activate the EMT signalling pathway of tumour cells, thereby promoting tumour invasion and migration.

4. Discussion

Although differences between right/left-sided tumours have been described, proteomics analysis of serum-derived EVs from RCC and LCC patients have not been reported. Previously, our team identified differences in the protein profile of serum-derived EVs from colon cancer patients compared with that of serum-derived EVs from healthy volunteers [20]. In addition, EVs form colon cancer patients promote cellular mobility of CRC cell line. In the current study, we discovered that the serum-derived EVs from RCC patients enhanced cellular invasion and migration more significantly than those derived from LCC patients. These results indicate that EVs derived from RCC patients contains more factors that are sufficient to promote metastasis. Proteomic profiles of these EVs and CRC cell lines treated with these EVs were obtained by TMT-based MS. The DEPs identified in serum EV were predicted to be involved in multiple processes and functions related to cancer progression, including tumour angiogenesis, epithelial cell migration, ECM remodelling and the TGF-β signalling pathway. Furthermore, DEPs identified from SW480 cells treated with different EVs were predominantly associated with the VEGFA-VEGFR2 signalling pathway and EMT in CRC. We hypothesize that serum-derived EVs from RCC patients promote metastasis by upregulation of ECM-related proteins, especially proteoglycans and glycoproteins, such as SPARC and LRG1.

Our study demonstrated that EVs derived from RCC patients contain a higher level of ECM-related proteins than those derived from LCC patients or healthy volunteers. Enrichment analysis showed that most of these ECM-related proteins are associated with ECM remodelling, which plays an important role in cell morphogenesis, survival, migration and invasion [30]. Several ECM proteins and the process of ECM remodelling are also implicated in regulating EMT [31], a process that contributes to the progression of tumour malignancy. Furthermore, aberrant ECM architecture has therapeutic consequences through its effects on drug penetration into the tumour [32]. Rahbari and colleagues reported a mechanism of acquired resistance to anti-VEGF therapy in liver mCRC and claimed a close correlation between ECM remodelling and resistance to anti-angiogenic therapy in liver

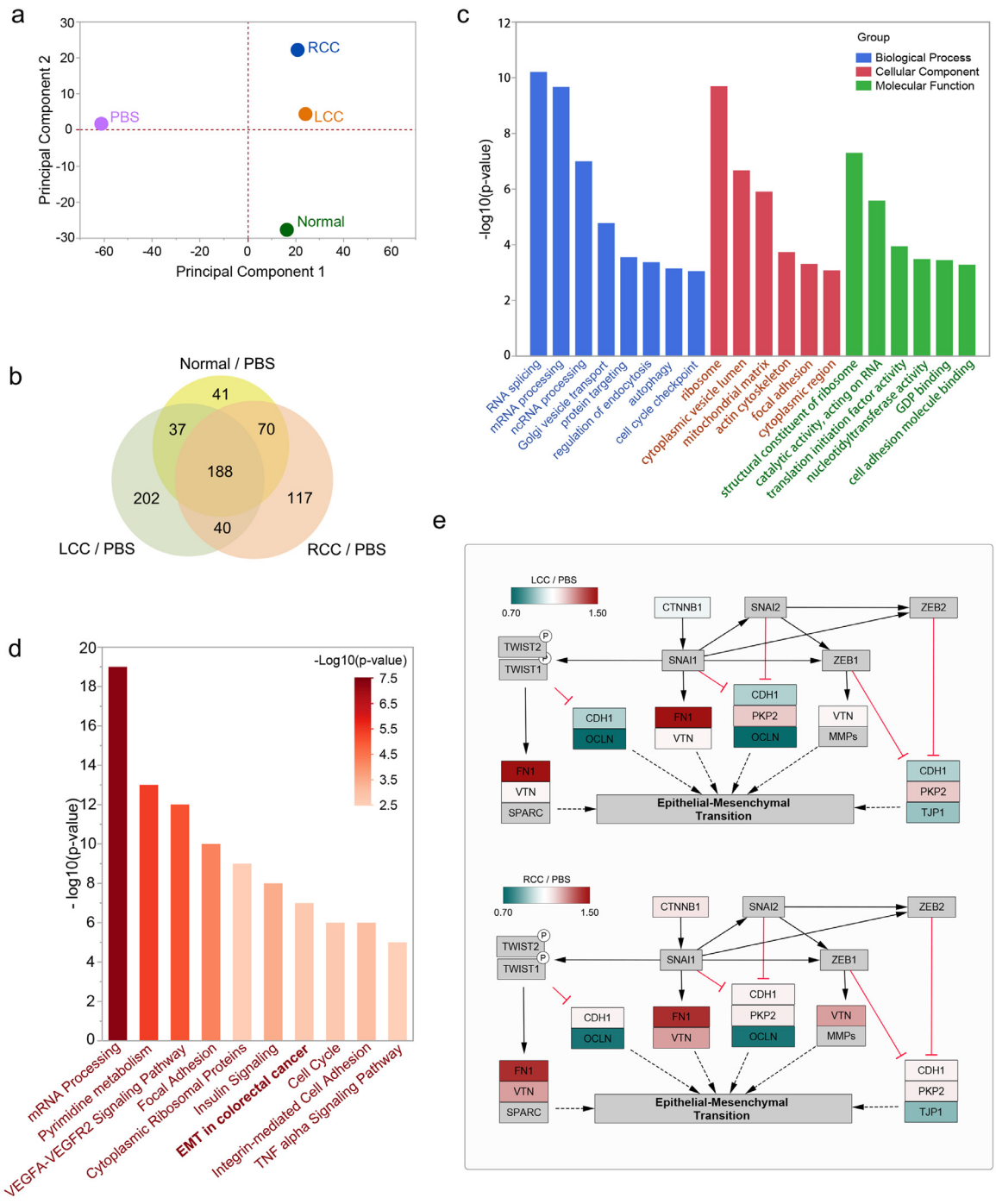

Fig. 6. Comparative analysis of proteome expression profiles of the SW480 cell line treated with different EV. (a) Principal component analysis revealed differences in the proteome profiles between RCC, LCC, normal groups, and PBS control. "LCC" refers to SW480 cells treated with EVs derived from patients with left-sided colon cancer. "RCC" refers to SW480 cells treated with EVs derived from patients with right-sided colon cancer. "Normal" refers to SW480 cells treated with EVs derived from healthy volunteers. "PBS" refers to SW480 cells treated with PBS. (b) Venn diagram showing the overlap of the groups of differentially expressed proteins between the Normal/PBS group (TMT-127/126), LCC/PBS group (TMT-129/126), and RCC/PBS group (TMT-131/126). (c) GO analysis of the cellular differentially expressed proteins. (d) Pathway analysis of the differentially expressed proteins. (e) The cellular differentially expressed proteins mapped to the EMT in CRC pathway (MS data presented as the ratios to 129/126 and 131/126). Up- or downregulation of identified proteins is indicated by colours in the pathway (upregulated in red, downregulated in green). (For interpretation of the references to colour in this figure legend, the reader is referred to the web version of this article.)

mCRC [33]. Combined with our findings, a higher level of ECM-related proteins may contribute to the poor efficacy of anti-EGFR therapy in stage IV RCC.

Among all the sidedness-associated DEPs, three ECM-related proteins (SPARC, VCAM1 and THBS1) were identified as hub proteins (Fig. 3g). All have been shown to play roles in angiogenesis and tumorigenesis. SPARC and VCAM1 were upregulated in RCC-derived EVs, while THBS1 was downregulated. SPARC is a multifunctional glycoprotein involved in cellular interactions in cell type- and context-dependent manner. Aberrant SPARC expression has been reported in various cancer types including melanoma, breast cancer, pancreatic cancer, and colorectal cancer [34–37]. SPARC regulates invasiveness, ECM remodelling, EMT, angiogenesis, cancer cell extravasation and metastasis, and response to tumour drug therapy [38–41]. For

Table 1
The top ten differentially expressed proteins of SW480 treated with serum EVs.

Accession	Gene Symbol	RCC/LCC*	Accession	Gene Symbol	RCC/LCC*
Q9GZZ9	UBA5	2.101	P69905	HBA1	1.384
P62304	SNRPE	1.534	Q9BYT8	NLN	1.365
Q96AX1	VPS33A	1.505	P62841	RPS15	1.364
Q5T0D9	TPRG1L	1.473	Q9Y2T3	GDA	1.362
Q9NZA1	CLIC5	1.455	Q8IUR7	ARMC8	1.359

*RCC/LCC: protein abundances ratio.

instance, high SPARC expression in the ECM is characteristic of tumours with increased EMT, and is associated with reduced treatment response and poor prognosis in high-grade breast cancer [37]. Moreover, SPARC modulates growth factor function and acts as an anti-adhesive factor in addition to interacting with several resident matrix proteins, including matrix metalloproteinases, which are also closely associated with EMT. SPARC was identified as a contributor to VCAM1-mediated leukocyte diapedesis, which is critical for recruitment of leukocytes to inflammatory sites. In melanoma, SPARC interacts with VCAM1 on endothelial cells to activate signalling pathways that increase endothelial paracellular permeability through disruption of intercellular junctions. This facilitates transmigration of tumour cells into the lung parenchyma [39]. THBS1 is known to be a critical negative regulator of tumour angiogenesis. In patients with oesophageal squamous cell carcinoma, low THBS1 expression is significantly associated with poor PFS [42]. Silencing of THBS1 leads to metastatic phenotypes in medulloblastoma [43]. In contrast, upregulating exosomal THBS1 inhibits lung cancer cell migration and invasion [44]. It can be speculated that decreased THBS1 expression, enhances angiogenesis in RCC.

Additionally, LRG1, a positive regulator of angiogenesis, was upregulated in RCC-derived EVs. As a novel pro-angiogenic factor, LRG1 has been reported to modulate angiogenesis and EMT in CRC via HIF-1α activation [29]. In the presence of TGF-β, LRG1 binds directly to the TGF-β accessory receptor endoglin to promote endothelial cell proliferation and migration via the pro-angiogenic Smad1/5/8 signalling pathway. Plasma LRG1 levels are reported to be higher in patients with CRC than in patients with adenomatous polyps, thus indicating the potential of LRG1 as a novel biomarker of the progression from colorectal adenoma to carcinoma [45]. Moreover, LRG1 with fucosylated triantennary N-glycan was identified as a new CRC marker, with a sensitivity and specificity exceeding CA19-9 [46].

Our study implies that serum-derived EVs from colon cancer patients promote cellular mobility and that CRC cells underwent EMT after treatment with such EVs (Fig. 6e). Increased expression of EMT markers, including FN1 and VTN, were observed in the RCC-EV-treated group, while only FN1 was upregulated in the LCC-EV-treated group. We suggest that EV proteins derived from colon cancer patients are involved in ECM remodelling and activation of EMT. As mentioned previously, LRG1 promotes EMT in CRC via HIF-1α activation, while SPARC regulates the expression of EMT-related genes, such as N-cadherin, vimentin, and FAM3C (interleukin-like EMT-inducer) [34]. In addition, SPARC enhances activation of the EMT signalling pathway via activation of AKT and acts as a mediator in the mechanism by which TGF-β1 promotes EMT [47,48].

In addition to its influence on EMT, SPARC binds to several integral components of the ECM and induces focal adhesion disassembly, thereby facilitating migration and invasion of metastatic cancer cells [49,50]. In accordance with this, various proteins associated with focal adhesion were found to be dysregulated after treatment with EVs derived from colon cancer patients.

Therefore, we hypothesize that both THBS1 downregulation and upregulation of SPARC and LRG1 induce tumour angiogenesis in RCC. Furthermore, SPARC and LRG1 promote metastasis by activation of ECM remodelling and EMT in CRC cells. Moreover, SPARC is required for the interactions of metastasizing CRC cells with circulating blood cells required to enable efficient extravasation across the vascular barrier. However, this hypothesis remains to be tested.

It is remarkable that the EV SPARC and LRG1 levels were higher in colon cancer patients than those in healthy control individuals. AUC values of 0.95 and 0.93, respectively, indicated that serum EV SPARC and LRG1 expression levels can be used to discriminate patients with colon cancer from healthy controls in a non-invasive manner. Both SPARC and LRG1 play pivotal roles in tumour progression. In accordance with this, the expression levels of SPARC and LRG1 were predictive of PFS and are therefore implicated as promising diagnostic and prognostic circulating biomarkers; however, this remains to be confirmed in a larger validation cohort.

We have perceived three limitations in this study. First, the EV isolation methods such as ultracentrifugation or Total Exosome Isolation Reagent can result in co-precipitation of proteins. Although we have washed the ultracentrifugation pellet with PBS in a mild approach, it can be not enough to remove the co-precipitation from proteins. Thus, our proteomic data might contain contamination. However, at least, the proteins that we used in this study are all listed in the EV database. Moreover, the EV level of LRG1 and SPARC were not parallel with the serum level (Fig. 5F; Fig. S5), which indicates that not all these proteins are originated from co-precipitation. Second, due to the limited number of patients enrolled in the early stage, long-term follow-up data are available for 30 patients only. Third, most of the healthy controls had not undergone a colonoscopy within the previous year. We are therefore not certain that if they have colon polyps. Further studies can be conducted to improve our understanding of the functional role of serum EVs in colon cancer.

5. Conclusion

In summary, the expression profile of the serum EV proteome in patients with RCC is different from that of patients with LCC. Serum-derived EVs of RCC promote metastasis more significant than those of LCC. This difference may be attributed to upregulation of EV ECM-related proteins, especially proteoglycans such as SPARC and glycoproteins such as LRG1. EV SPARC and LRG1 are potential non-invasive diagnostic and prognostic biomarkers in colon cancer.

Data sharing

The MS proteomics datasets are available from the ProteomeXchange Consortium with the identifier PXD012283 and PXD012304.

Declaration of competing interest

The authors have declared that no competing interest exists.

Acknowledgments

We would like to thank our lab colleagues for their support in the development of this article. We are also grateful to this article's reviewers and editor.

Funding sources

This work was supported by the CAMS Innovation Fund for Medical Sciences (No. 2017-I2M-1–009); the Fundamental Research Funds for the Central Universities (No. 3332018136); Peking Union Medical College Graduate Student Innovation Fund (2017–1002–2–25); the National Natural Science Foundation of China (No. 81702933). The funders had no role in study design, data collection, data analysis and interpretation, preparation of the manuscript, or decision to publish.

Author contributions

Conception and design: M. Zhong, W. Ge, B. Wu
Development of methodology: W. Ge, M. Zhong, Y. Chen
Acquisition of data: M. Zhong, Y. Chen, Y. Xiao, L. Xu, G. Zhang, J. Lu, H. Qiu, W. Ge, B. Wu
Analysis and interpretation of data: M. Zhong, W. Ge
Writing, review, and/or revision of the manuscript: M. Zhong, W. Ge, B. Wu, Y. Chen
Administrative, technical, or material support: W. Ge, Y. Chen
Study supervision: W. Ge, B. Wu

Supplementary materials

Supplementary material associated with this article can be found in the online version at doi:10.1016/j.ebiom.2019.11.003.

References

[1] Imperial R, Ahmed Z, Toor OM, Erdogan C, Khaliq A, Case P, et al. Comparative proteogenomic analysis of right-sided colon cancer, left-sided colon cancer and rectal cancer reveals distinct mutational profiles. Mol Cancer 2018;17(1):177.
[2] Boeckx N, Koukakis R, Op de Beeck K, Rolfo C, Van Camp G, Siena S, et al. Primary tumor sidedness has an impact on prognosis and treatment outcome in metastatic colorectal cancer: results from two randomized first-line panitumumab studies. Ann Oncol 2017;28(8):1862–8.
[3] 5475 AB, Venook AP, Cederquist L, Chan E, Chen Y-J, Cooper HS, et al. Colon cancer, version 1.2017, NCCN clinical practice guidelines in oncology. J Natl Comprehens Cancer Netw 2017;15(3):370–98.
[4] Park JH, Kim MJ, Park SC, Kim MJ, Hong CW, Sohn DK, et al. Difference in time to locoregional recurrence between patients with right-sided and left-sided colon cancers. Dis Colon Rectum 2015;58(9):831–7.
[5] Arnold D, Lueza B, Douillard JY, Peeters M, Lenz HJ, Venook A, et al. Prognostic and predictive value of primary tumour side in patients with RAS wild-type metastatic colorectal cancer treated with chemotherapy and EGFR directed antibodies in six randomized trials. Ann Oncol 2017;28(8):1713–29.
[6] Brulé SY, Jonker DJ, Karapetis CS, O'Callaghan CJ, Moore MJ, Wong R, et al. Location of colon cancer (right-sided versus left-sided) as a prognostic factor and a predictor of benefit from cetuximab in NCIC CO.17. Eur J Cancer 2015;51(11):1405–14.
[7] Tejpar S, Stintzing S, Ciardiello F, Tabernero J, Van Cutsem E, Beier F, et al. Prognostic and predictive relevance of primary tumor location in patients with RAS wild-type metastatic colorectal cancer: retrospective analyses of the crystal and FIRE-3 trials. JAMA Oncol 2016.
[8] Venook AP, Niedzwiecki D, Innocenti F, Fruth B, Greene C, O'Neil BH, et al. Impact of primary (1°) tumor location on overall survival (OS) and progression-free survival (PFS) in patients (pts) with metastatic colorectal cancer (mCRC): analysis of CALGB/SWOG 80405 (4254). J Clin Oncol 2017.
[9] Loupakis F, Yang D, Yau L, Feng S, Cremolini C, Zhang W, et al. Primary tumor location as a prognostic factor in metastatic colorectal cancer. J Natl Cancer Inst 2015;107(3).
[10] Zhong M-E, Wu B, Xu L, Xiao Y, Lin G-L, Qiu H-Z. Comparison of clinicopathologic features and survival between patients with right-sided and left-sided stage III colon cancer. Transl Cancer Res 2017;6(1):254–60.
[11] Taieb J, Kourie HR, Emile JF, Le Malicot K, Balogoun R, Tabernero J, et al. Association of prognostic value of primary tumor location in stage III colon cancer with RAS and BRAF mutational status. JAMA Oncol 2018;4(7):e173695.
[12] Shah R, Patel T, Freedman JE. Circulating extracellular vesicles in human disease. N Engl J Med 2018;379(10):958–66.
[13] Hoshino A, Costa-Silva B, Shen TL, Rodrigues G, Hashimoto A, Tesic Mark M, et al. Tumour exosome integrins determine organotropic metastasis. Nature 2015;527(7578):329–35.
[14] Mathieu M, Martin-Jaular L, Lavieu G, Thery C. Specificities of secretion and uptake of exosomes and other extracellular vesicles for cell-to-cell communication. Nat Cell Biol 2019;21(1):9–17.
[15] Zomer A, Maynard C, Verweij FJ, Kamermans A, Schafer R, Beerling E, et al. *In vivo* imaging reveals extracellular vesicle-mediated phenocopying of metastatic behavior. Cell. 2015;161(5):1046–57.
[16] Zhang L, Zhang S, Yao J, Lowery FJ, Zhang Q, Huang WC, et al. Microenvironment-induced PTEN loss by exosomal microRNA primes brain metastasis outgrowth. Nature 2015;527(7576):100–4.
[17] Syn N, Wang L, Sethi G, Thiery JP, Goh BC. Exosome-mediated metastasis: from epithelial-mesenchymal transition to escape from immunosurveillance. Trends Pharmacol Sci 2016;37(7):606–17.
[18] Xiao D, Barry S, Kmetz D, Egger M, Pan J, Rai SN, et al. Melanoma cell-derived exosomes promote epithelial-mesenchymal transition in primary melanocytes through paracrine/autocrine signaling in the tumor microenvironment. Cancer Lett 2016;376(2):318–27.
[19] Provenzale D, Jasperson K, Ahnen DJ, Aslanian H, Bray T, Cannon JA, et al. Colorectal cancer screening, version 1.2015. J Natl Comprehens Cancer Netw 2015;13(8):959–68.
[20] Chen Y, Xie Y, Xu L, Zhan S, Xiao Y, Gao Y, et al. Protein content and functional characteristics of serum-purified exosomes from patients with colorectal cancer revealed by quantitative proteomics. Int J Cancer 2017;140(4):900–13.
[21] Cottrell JS. Protein identification using MS/MS data. J Proteomics 2011;74(10):1842–51.
[22] Deutsch EW, Csordas A, Sun Z, Jarnuczak A, Perez-Riverol Y, Ternent T, et al. The ProteomeXchange consortium in 2017: supporting the cultural change in proteomics public data deposition. Nucleic Acids Res 2017;45(D1):D1100–D6.
[23] Uhlen M, Fagerberg L, Hallstrom BM, Lindskog C, Oksvold P, Mardinoglu A, et al. Proteomics. Tissue-based map of the human proteome. Science 2015;347(6220):1260419.
[24] Yu G, Wang LG, Han Y, He QY. clusterProfiler: an R package for comparing biological themes among gene clusters. OMICS 2012;16(5):284–7.
[25] Bindea G, Mlecnik B, Hackl H, Charoentong P, Tosolini M, Kirilovsky A, et al. ClueGO: a Cytoscape plug-in to decipher functionally grouped gene ontology and pathway annotation networks. Bioinformatics 2009;25(8):1091–3.
[26] Szklarczyk D, Morris JH, Cook H, Kuhn M, Wyder S, Simonovic M, et al. The STRING database in 2017: quality-controlled protein-protein association networks, made broadly accessible. Nucleic Acids Res 2017;45(D1):D362–D8.
[27] Cline MS, Smoot M, Cerami E, Kuchinsky A, Landys N, Workman C, et al. Integration of biological networks and gene expression data using Cytoscape. Nat Protoc 2007;2(10):2366–82.
[28] Sansom OJ, Mansergh FC, Evans MJ, Wilkins JA, Clarke AR. Deficiency of SPARC suppresses intestinal tumorigenesis in APCMin/+ mice. Gut 2007;56(10):1410–4.
[29] Zhang J, Zhu L, Fang J, Ge Z, Li X. LRG1 modulates epithelial-mesenchymal transition and angiogenesis in colorectal cancer via HIF-1alpha activation. J Exp Clin Cancer Res 2016;35:29.
[30] Zaman MH, Trapani LM, Sieminski AL, Mackellar D, Gong H, Kamm RD, et al. Migration of tumor cells in 3D matrices is governed by matrix stiffness along with cell-matrix adhesion and proteolysis. Proc Natl Acad Sci U S A 2006;103(29):10889–94.
[31] Hoshiba T. An extracellular matrix (ECM) model at high malignant colorectal tumor increases chondroitin sulfate chains to promote epithelial-mesenchymal transition and chemoresistance acquisition. Exp Cell Res 2018;370(2):571–8.
[32] Provenzano PP, Cuevas C, Chang AE, Goel VK, Von Hoff DD, Hingorani SR. Enzymatic targeting of the stroma ablates physical barriers to treatment of pancreatic ductal adenocarcinoma. Cancer Cell 2012;21(3):418–29.
[33] Rahbari NN, Kedrin D, Incio J, Liu H, Ho WW, Nia HT, et al. Anti-VEGF therapy induces ECM remodeling and mechanical barriers to therapy in colorectal cancer liver metastases. Sci Transl Med 2016;8(360) 360ra135.
[34] Girotti MR, Fernandez M, Lopez JA, Camafeita E, Fernandez EA, Albar JP, et al. SPARC promotes cathepsin B-mediated melanoma invasiveness through a collagen I/alpha2beta1 integrin axis. J Invest Dermatol 2011;131(12):2438–47.
[35] Nagathihalli NS, Castellanos JA, Shi C, Beesetty Y, Reyzer ML, Caprioli R, et al. Signal transducer and activator of transcription 3, mediated remodeling of the tumor microenvironment results in enhanced tumor drug delivery in a mouse model of pancreatic cancer. Gastroenterology 2015;149(7):1932–43 e9.
[36] Kaiser S, Park YK, Franklin JL, Halberg RB, Yu M, Jessen WJ, et al. Transcriptional recapitulation and subversion of embryonic colon development by mouse colon tumor models and human colon cancer. Genome Biol 2007;8(7):R131.
[37] Sangaletti S, Tripodo C, Santangelo A, Castioni N, Portararo P, Gulino A, et al. Mesenchymal transition of high-grade breast carcinomas depends on extracellular matrix control of myeloid suppressor cell activity. Cell Rep 2016;17(1):233–48.
[38] Tanaka HY, Kitahara K, Sasaki N, Nakao N, Sato K, Narita H, et al. Pancreatic stellate cells derived from human pancreatic cancer demonstrate aberrant SPARC-dependent ECM remodeling in 3D engineered fibrotic tissue of clinically relevant thickness. Biomaterials 2018;192:355–67.
[39] Tichet M, Prod'Homme V, Fenouille N, Ambrosetti D, Mallavialle A, Cerezo M, et al. Tumour-derived SPARC drives vascular permeability and extravasation through endothelial VCAM1 signalling to promote metastasis. Nat Commun 2015;6:6993.
[40] Lindner JL, Loibl S, Denkert C, Ataseven B, Fasching PA, Pfitzner BM, et al. Expression of secreted protein acidic and rich in cysteine (SPARC) in breast cancer and response to neoadjuvant chemotherapy. Ann Oncol 2015;26(1):95–100.
[41] Sinn M, Sinn BV, Striefler JK, Lindner JL, Stieler JM, Lohneis P, et al. SPARC expression in resected pancreatic cancer patients treated with gemcitabine: results from the CONKO-001 study. Ann Oncol 2014;25(5):1025–32.
[42] Tzeng HT, Tsai CH, Yen YT, Cheng HC, Chen YC, Pu SW, et al. Dysregulation of Rab37-mediated cross-talk between cancer cells and endothelial cells via thrombospondin-1 promotes tumor neovasculature and metastasis. Clin Cancer Res 2017;23(9):2335–45.
[43] Zhou L, Picard D, Ra YS, Li M, Northcott PA, Hu Y, et al. Silencing of thrombospondin-1 is critical for myc-induced metastatic phenotypes in medulloblastoma. Cancer Res 2010;70(20):8199–210.
[44] Huang WT, Chong IW, Chen HL, Li CY, Hsieh CC, Kuo HF, et al. Pigment epithelium-derived factor inhibits lung cancer migration and invasion by upregulating exosomal thrombospondin 1. Cancer Lett 2018;442:287–98.

[45] Choi J-W, Liu H, Shin DH, Yu GI, Hwang JS, Kim ES, et al. Proteomic and cytokine plasma biomarkers for predicting progression from colorectal adenoma to carcinoma in human patients. Proteomics 2013;13(15):2361–74.
[46] Shinozaki E, Tanabe K, Akiyoshi T, Tsuchida T, Miyazaki Y, Kojima N, et al. Serum leucine-rich alpha-2-glycoprotein-1 with fucosylated triantennary N-glycan: a novel colorectal cancer marker. BMC Cancer 2018;18(1):406.
[47] Sun W, Feng J, Yi Q, Xu X, Chen Y, Tang L. SPARC acts as a mediator of TGF-beta1 in promoting epithelial-to-mesenchymal transition in A549 and H1299 lung cancer cells. Biofactors 2018;44(5):453–64.
[48] Chang CH, Yen MC, Liao SH, Hsu YL, Lai CS, Chang KP, et al. Secreted protein acidic and rich in cysteine (SPARC) enhances cell proliferation, migration, and epithelial mesenchymal transition, and SPARC expression is associated with tumor grade in head and neck cancer. Int J Mol Sci 2017;18(7).
[49] Nagaraju GP, Dontula R, El-Rayes BF, Lakka SS. Molecular mechanisms underlying the divergent roles of SPARC in human carcinogenesis. Carcinogenesis 2014;35(5):967–73.
[50] Brekken RA, Sage EH. SPARC, a matricellular protein: at the crossroads of cell–matrix communication. Matrix Biol 2001;19(8):815–27.